Electronic Supplementary Material (ESI) for Soft Matter.
This journal is © The Royal Society of Chemistry 2018

Supporting Information—Spin-echo small-angle neutron scattering (SESANS) studies of diblock copolymer nanoparticles

Gregory N. Smith,[*,†,‡] Victoria J. Cunningham,[†,¶] Sarah L. Canning,[†,§] Matthew J. Derry,[†] J. F. K. Cooper,[‖] A. L. Washington,[‖] and Steven P. Armes[†]

†*University of Sheffield, Department of Chemistry, Dainton Building, Brook Hill, Sheffield, South Yorkshire, S3 7HF, United Kingdom*

‡*Present address: Niels Bohr Institute, University of Copenhagen, Universitetsparken 5, 2100 Copenhagen Ø, Denmark*

¶*Present address: Scott Bader Company Ltd., Wollaston, NN29 7RL, United Kingdom*

§*Present address: Fujifilm Speciality Ink Systems Ltd, Pysons Road, Broadstairs, Kent CT10 2LE, United Kingdom*

‖*ISIS-STFC, Rutherford Appleton Laboratory, Chilton, Oxon OX11 0QX, United Kingdom*

E-mail: gregory.smith@nbi.ku.dk

PGMA–PBzMA diblock copolymer characterization

Gel permeation chromatography (GPC)

The molar masses and dispersities of the PGMA macro-CTA and PGMA–PBzMA diblock copolymers were determined by DMF GPC at 60 °C. The GPC set-up consisted of two Polymer Laboratories PL gel 5 μm Mixed C columns connected in series to a Varian 390 LC multidetector suite (refractive index detector) and a Varian 290 LC pump injection module. The mobile phase was HPLC grade DMF containing 10 mmol LiBr with a flow rate of 1.0 mL min^{-1}. Copolymer solutions (1.0% wt/vol) were prepared in DMF using DMSO as the flow rate marker. Ten near-monodisperse PMMA standards (M_n = 625 to 618 000 g mol^{-1}) were used for calibration. Data were analyzed using Varian Cirrus GPC software (version 3.3).

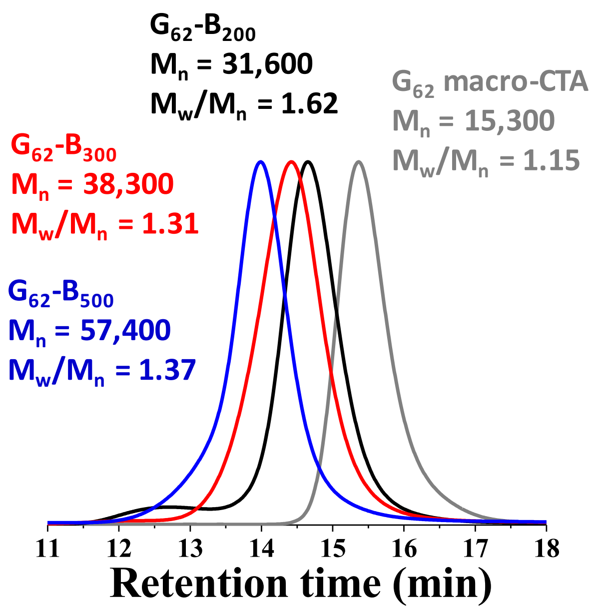

Figure S1: DMF GPC chromatograms for PGMA$_{62}$–PBzMA$_x$ (G$_{62}$–B$_x$) diblock copolymers.

Dynamic light scattering (DLS)

DLS measurements were performed using a Malvern Zetasizer NanoZS instrument. Aqueous dispersions (0.20% wt/wt) were analyzed using disposable plastic cuvettes and data were averaged over three consecutive runs. Z-average diameters (d_Z) and intensity diameters (d_I) were calculated in the instrument software directly from the correlogram. Volume diameters (d_V) were calculated from the intensity diameter in the instrument software using Mie theory with the particle refractive index set to that of poly(benzyl methacrylate) ($n = 1.568$).[1]

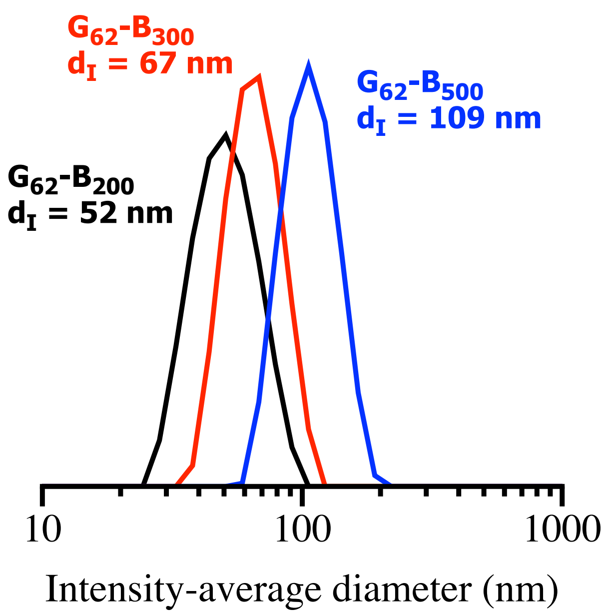

Figure S2: Intensity particle size distributions of $PGMA_{62}$–$PBzMA_x$ (G_{62}–B_x) nanoparticles.

Table S1: $PGMA_{62}$–$PBzMA_x$ diameters from DLS data.

	d_Z / nm	Polydispersity index	d_I / nm	σ_I / nm	d_V / nm	σ_V / nm
$PGMA_{62}$–$PBzMA_{200}$	48	0.06	52	14	43	12
$PGMA_{62}$–$PBzMA_{300}$	64	0.02	67	15	58	15
$PGMA_{62}$–$PBzMA_{500}$	104	0.02	109	25	98	26

Transmission electron microscopy (TEM)

Copper/palladium TEM grids (Agar Scientific) were coated in-house to yield a thin film of amorphous carbon. The grids were then subjected to a glow discharge for 30 s to create a hydrophilic surface. Individual samples (0.20% wt/wt aqueous dispersion, 10.0 μL) were adsorbed onto the freshly-treated grids for 1 min and then blotted with filter paper to remove excess solution. To stain the colloidal aggregates, uranyl formate (9.0 μL of a 0.75% wt/wt solution) was absorbed onto the sample-loaded grid for 20 s and then carefully blotted to remove excess stain. The grids were then dried using a vacuum hose. Imaging was performed using a Philips CM100 instrument operating at 100 kV and equipped with a Gatan 1 k CCD camera.

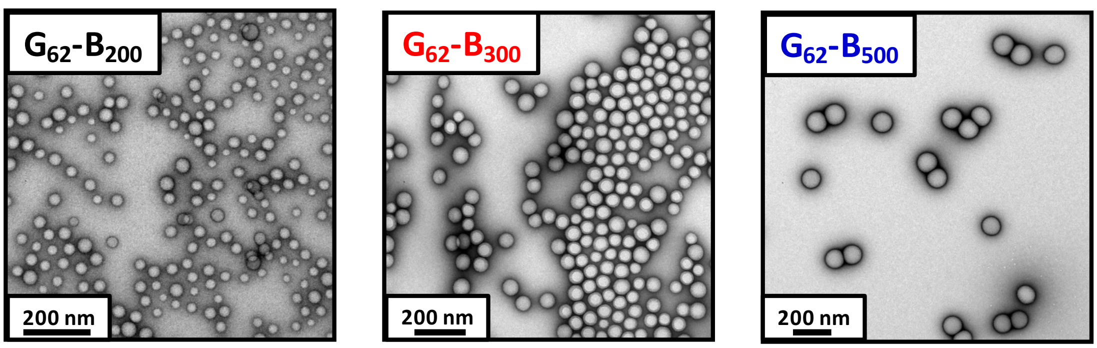

(a) $PGMA_{62}$–$PBzMA_{200}$ (b) $PGMA_{62}$–$PBzMA_{300}$ (c) $PGMA_{62}$–$PBzMA_{500}$

Figure S3: TEM images of $PGMA_{62}$–$PBzMA_x$ diblock copolymer micelles. All are found to form spherical nanoparticles.

Summary of properties of $PGMA_{62}$–$PBzMA_x$ diblock copolymer nanoparticles

Table S2: Summary of the analyses of $PGMA_{62}$–$PBzMA_x$ diblock copolymer nanoparticles in solution.

	BzMA Conversion	M_n / (g mol^{-1})	$Đ_M$
$PGMA_{62}$ macromolecular CTA	—	15,300	1.15
$PGMA_{62}$–$PBzMA_{200}$	$> 99\%$	31,600	1.62
$PGMA_{62}$–$PBzMA_{300}$	$> 99\%$	38,300	1.31
$PGMA_{62}$–$PBzMA_{500}$	$> 99\%$	57,400	1.37

PGMA–PBzMA diblock copolymers in H_2O and D_2O

The intensity diameters for the three $PGMA_{62}$–$PBzMA_x$ diblock copolymer micelles synthesized in this study have been compared to those measured for $PGMA_{51}$–$PBzMA_x$ diblock copolymers reported in the literature.[2] For exclusively sphere-forming systems, radii should vary as a power law function of the core DP. Despite small differences in the radii found in H_2O and in D_2O, the radii do vary as a power law in DP, further confirming that spheres are the dominant morphology.

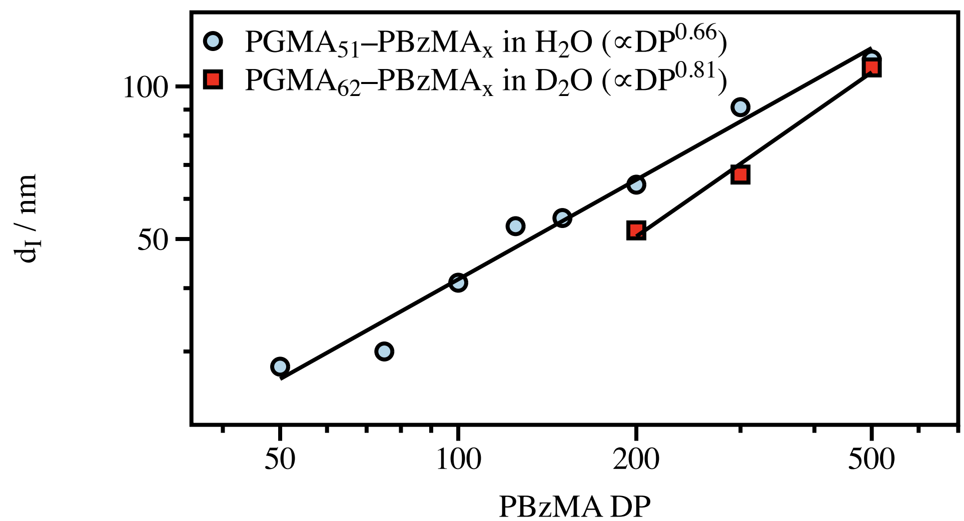

Figure S4: Intensity diameters (d_I) of two sets of PGMA–PBzMA diblock copolymer micelles synthesized in H_2O ($PGMA_{51}$ stabilizer)[2] from the literature and in D_2O ($PGMA_{62}$) from this study.

SAXS model

The scattering cross section per unit volume from a dispersion of homogeneous nanoparticles ($\mathrm{d}\Sigma/\mathrm{d}\Omega(Q)$), equivalently referred to as the intensity ($I(Q)$), can be given by the following expression, where $P(Q)$ is the form factor, $S(Q)$ is the structure factor, n is the number density, ϕ is the volume fraction, V_t is the volume of the object, and $\Delta\rho$ is the contrast between solvent and solute.

$$\frac{\mathrm{d}\Sigma}{\mathrm{d}\Omega}(Q) \equiv I(Q) = nV_t^2\Delta\rho^2 P(Q)S(Q) = \phi V_t \Delta\rho^2 S(Q)P(Q) \tag{S1}$$

$P(Q)$ is related to the geometry of the scattering object. For composite objects, such as polymer micelles, $P(Q)$ depends on the scattering length density (SLD, ρ) difference between parts of the system as well as their volume, so is a function of both. $S(Q)$ accounts for deviations from a random distribution of scattering objects, which only become appreciable for either concentrated dispersions or for strongly interacting species. The SAXS data reported here are for dilute dispersions, and in this case, $S(Q) = 1$.

The spherical nanoparticles studied here are diblock copolymer micelles, and the form factors of these have previously been reported in the literature.[3,4] The form factor (P_m) of a spherical diblock copolymer micelle consists of four terms: two self-terms (for the spherical core, P_s, and the chains on the surface, P_c) and two cross-terms (between the core and the chains, S_{sc}, and between different chains on the surface, S_{cc}).

$$P_m(Q) = N^2\beta_s^2 P_s(Q) + N\beta_c^2 P_c(Q) + 2N^2\beta_s\beta_c S_{sc}(Q) + N(N-1)\beta_c^2 S_{cc}(Q) \tag{S2}$$

Unlike for homogenous particles, the form factor depends on the volumes and scattering length densities of the blocks. N is the aggregation number, and β_s and β_c are the total excess scattering lengths of blocks in the core and the shell, respectively. They are given by $\beta_s = V_s(\rho_s - \rho_m)$ and $\beta_c = V_c(\rho_c - \rho_m)$, where V is the volume of a block and ρ is the scattering length density of a block. ρ_m is the scattering length density of the solvent medium.

The form factor for the self-term is simply the well-known spherical form factor for a sphere of radius r.[5,6]

$$P_s(Q) = \left[\frac{3 \left[\sin{(Qr)} - Qr \cos{(Qr)} \right]}{(Qr)^3} \right]^2 \tag{S3}$$

The self-term for the chains in the corona given by the Debye function, assuming that they are Gaussian chains with a radius of gyration R_g.[7]

$$P_c(Q) = \frac{2 \left[\exp{(-Q^2 R_g^2)} - 1 + Q^2 R_g^2 \right]}{Q^4 R_g^4} \tag{S4}$$

To mimic non-penetration of the Gaussian chains, they are set as starting a distance dR_g away from the surface of the core, where $d \approx 1$. The cross-term between core and chains is given by the following expression.

$$S_{sc}(Q) = \Phi(Qr)\psi(QR_g) \frac{\sin{(Q \left[r + dR_g \right])}}{Q \left[r + dR_g \right]} \tag{S5}$$

The functions $\Phi(x)$ and $\psi(x)$ are given below.

$$\Phi(x) = \frac{3 \left[\sin{(x)} - Qr \cos{(x)} \right]}{(x)^3} \tag{S6}$$

$$\psi(x) = \frac{\left[1 - \exp{(-x)} \right]}{x} \tag{S7}$$

The interference term between chains in the corona is given by the following expression.

$$S_{cc}(Q) = \psi^2(QR_g) \left[\frac{\sin{(Q \left[r + dR_g \right])}}{Q \left[r + dR_g \right]} \right]^2 \tag{S8}$$

The model as implemented in SasView does not include a distribution in the radius of the core. The fit radii have been compared to a modified spherical diblock copolymer micelle model (including a sigmoidal interface to account for a varying scattering length density at the micellar interface and a radial profile to define scattering in the micelle corona using a linear combination of two cubic splines with fitting parameters corresponding to the width and weight coefficient).[8–10] The fit radii from the two approaches compare favorably.

SAXS data fitting

SAXS data were fit to models as explained in the previous sections. Geometric parameters (core r and corona block R_g) were allowed to vary, and the volumes and SLDs of the two blocks were fixed from the known mass densities of the materials.

Table S3: Mass densities of materials

	Mass density / (g cm^{-3})
PGMA[11]	1.310
PBzMA[1]	1.179
D_2O[1]	1.107

Using this mass density and the molar mass of the species, the molecular volume (V_m) of the polymer blocks can be calculated.

Table S4: Molecular volumes of polymer blocks

	PGMA block V_m / Å^3	PBzMA V_m / Å^3
$PGMA_{62}$–$PBzMA_{200}$	12584	49636
$PGMA_{62}$–$PBzMA_{300}$	12584	74455
$PGMA_{62}$–$PBzMA_{500}$	12584	124091

To calculate the scattering length densities, both the coherent scattering length (b_i) and the molar volumes must be known.

$$\rho = \frac{\sum_i b_i}{V_m} \tag{S9}$$

For X-rays, as scattering arises from the interaction between X-rays and the atomic electron cloud, b_i is related to the atomic number (Z). At X-ray energies away from absorption edges, the atomic scattering factor f_1 is well approximated by the Z. In this case, b_i is equal to the product of the atomic number and the classical electron radius (r_e).[12,13]

These values were fixed in the models, and the geometric parameters allowed to vary. The best fit values are given in Table S6.

Table S5: X-ray scattering length densities of materials

	ρ_X / (10^{-6} Å^{-2})
PGMA	11.9
PBzMA	10.7
D_2O	9.39

Table S6: SAXS fitting parameters

	Core r / Å	PGMA R_g / Å
$PGMA_{62}$–$PBzMA_{200}$	179.3	20.7
$PGMA_{62}$–$PBzMA_{300}$	256.3	18.5
$PGMA_{62}$–$PBzMA_{500}$	437.8	16.5

SESANS model

The SESANS technique has been well described elsewhere, and interested readers are directed to these articles for more information.[14–16] In the following section, important aspects of the scattering theory and data analysis of SESANS measurements are discussed. In general, as opposed to conventional SAS measurements that measure scattering intensity as a function of momentum transfer (the magnitude of the vector $\vec{Q}$), SESANS measurements the degree of depolarization as a function of correlation length. This parameter is called the spin echo length Z, essentially the correlation distance probed in the sample.

In a SESANS measurement, the average polarization of a neutron beam that has passed through a sample is the quantity that is being measured. The unscattered beam retains its original polarization ($P_0(Z)$), and the scattered beam is partly depolarized ($P(Z)$). The degree of depolarization is given in Equation S10.

$$\frac{P(Z)}{P_0(Z)} = \exp\left\{\Sigma_t \left[G(Z) - 1\right]\right\} \tag{S10}$$

Σ_t is the average number of scattering events for a neutron passing through a sample of thickness t, and $G(Z)$ is a correlation function that is related, via an Abel transform, to a Debye-type autocorrelation function $\gamma(r)$.[15–17] $G(Z)$ is given in Equation S11.

$$G(Z) = \frac{2}{\xi} \int_z^\infty \frac{\gamma(r) r}{\left(r^2 - z^2\right)^{1/2}} \mathrm{d}r \tag{S11}$$

In Equation S11, ξ is a normalizing constant.

$$\xi = 2 \int_0^\infty \gamma(r) \mathrm{d}r \tag{S12}$$

The total scattering scales as a function of the square of the neutron wavelength (λ^2) and linearly with the sample thickness (t). Therefore, the following quantity has emerged as a useful y-axis for SESANS measurements.

$$\frac{1}{\lambda^2 t}\ln\left[\frac{P(Z)}{P_0(Z)}\right] \tag{S13}$$

It has been proposed to refer to it as "the wavelength and sample-thickness normalized SESANS signal" or simply "the normalized SESANS signal".[16] We will use the latter name.

For isotropically scattering samples, as is the case for the spheres used in this study, $G(Z)$ can be related to the scattering cross section per unit volume ($\mathrm{d}\sigma/\mathrm{d}\Omega$) encountered in a conventional SAS measurement, as shown in Equation S14. $J_0(x)$ is the zeroth order cylindrical Bessel function.

$$G(Z) = \frac{\lambda^2 t}{2\pi\Sigma_t}\int_0^\infty J_0(Qz)\frac{\mathrm{d}\sigma}{\mathrm{d}\Omega}(Q)Q\mathrm{d}Q \tag{S14}$$

The scattering cross section can be related to the quantity $I(Q)$, as defined by Andersson *et al.*[15] Note that this quantity is carefully defined by Andersson *et al.* and *is not* equivalent to the identically named quantity typically used by small-angle scattering practitioners, as is the case in this study, to be the scattering cross section per unit volume (Equation S1). In the nomenclature of Andersson *et al.*, the relationship between $\mathrm{d}\sigma/\mathrm{d}\Omega$ and $I(Q)$ is given by Equation S15.

$$\frac{\mathrm{d}\sigma}{\mathrm{d}\Omega} = \langle\rho^2\rangle I(Q) \tag{S15}$$

The quantity $\langle\rho^2\rangle$ is the average of the square of the difference in SLD between the dispersed and continuous phases, as defined by Feigin and Svergun,[18] where ϕ_i is the volume fraction and ρ_i is the SLD of the i^{th} component.

$$\langle\rho^2\rangle = \sum_{i\neq j}\phi_i\phi_j\left(\rho_i - \rho_j\right)^2 \tag{S16}$$

Using the nomenclature of Andersson *et al.* for $I(Q)$ (Equation S15), this quantity can be expressed in terms of parameters also encountered in conventional SAS measurements: the volume fraction (ϕ), the particle volume (V_t), the structure factor ($S(Q)$), and the square root of the form factor ($F(Q)$).

$$I(Q) = \frac{1}{(1-\phi)V_t} S(Q) \left|F(Q)\right|^2 \tag{S17}$$

The form factor ($P(Q)$) was previously given (Equation S3), as this is the self-term for the spherical polymer micelle model. The square root form ($F(Q)$) is given in Equation S18.

$$F(Q) = \frac{3\left[\sin(Qr) - Qr\cos(Qr)\right]}{(Qr)^3} \tag{S18}$$

The model used to fit the SESANS data treats the interparticle interactions with a hard sphere $S(Q)$, details of which can be found in the original publication by Percus and Yevick.[19]

Finally, the total single scattering probability (Σ_t) is given by Equation S19.[15]

$$\Sigma_t = \frac{\lambda^2 t}{2\pi} \int_0^\infty \frac{\mathrm{d}\sigma}{\mathrm{d}\Omega}(Q) Q \mathrm{d}Q = \frac{\lambda^2 t}{2\pi} \langle \rho^2 \rangle \int_0^\infty I(Q) Q \mathrm{d}Q = \lambda^2 t \langle \rho^2 \rangle \xi \tag{S19}$$

Using the normalized SESANS signal (Equation S13), it is possible to determine $G(Z)$ and and Σ_t independently from measurements of $P(Z)$ and $P_0(Z)$, as shown in the equations below.

$$G(Z) = 1 - \frac{\ln\left[\frac{P(Z)}{P_0(Z)}\right]}{\ln\left[\frac{P(\infty)}{P_0(\infty)}\right]} \tag{S20}$$

$$\ln\left[\frac{P(\infty)}{P_0(\infty)}\right] = -\Sigma_t \tag{S21}$$

For homogeneously scattering particles, as is the case in this study, the correlation function and the total scattering cross section can be analyzed independently. $G(Z)$ provides information about interparticle correlations, and Σ_t provides information about the SLD contrast and the average correlation distance.

SESANS fitting

The materials used are the same as for the SAXS analysis, and therefore, the mass densities and molecular volumes are identical (Tables S3 and S4). Unlike X-rays, which interact with atomic electron clouds, neutrons interact with atomic nuclei, and the molecular scattering length b_i and scattering length density ρ must be calculated using neutron atomic scattering lengths. These have been tabulated by Sears[20] or are available elsewhere.[21] Otherwise, SLDs can be calculated identically as for X-rays using Equation S9.

Table S7: Neutron scattering length densities of materials

	ρ_n / (10^{-6} Å^{-2})
PGMA	1.23
PBzMA	1.61
D_2O	6.38

The SLDs were initially set to the values in Table S7, although they were allowed to vary. The volume fraction ϕ and the scale factor (equal to $(1-\phi)$) were treated as fitting parameters. The fit volume fractions were found to be less than expected from sample preparation ($\phi = 0.28$), and this merits further study on more concentrated dispersions in the future. The sums of the fit volume fraction and scale give values near to 1 (ranging from 0.99 to 1.09), as would be expected. The best fit values are shown in Table S8.

Table S8: SESANS fitting parameters

	r / Å	ρ / (10^{-6} Å^{-2})	ϕ
$PGMA_{62}$–$PBzMA_{200}$	308	4.35	0.26
$PGMA_{62}$–$PBzMA_{300}$	332	3.31	0.23
$PGMA_{62}$–$PBzMA_{500}$	485	2.00	0.14

References

(1) Sigma–Aldrich. http://www.sigmaaldrich.com/united-kingdom.html.

(2) Cunningham, V. J.; Alswieleh, A. M.; Thompson, K. L.; Williams, M.; Leggett, G. J.; Armes, S. P.; Musa, O. M. Poly(glycerol monomethacrylate)–Poly(benzyl methacrylate) Diblock Copolymer Nanoparticles via RAFT Emulsion Polymerization: Synthesis, Characterization, and Interfacial Activity. *Macromolecules* **2014**, *47*, 5613–5623.

(3) Pedersen, J. S.; Gerstenberg, M. C. Scattering Form Factor of Block Copolymer Micelles. *Macromolecules* **1996**, *29*, 1363–1365.

(4) Pedersen, J. S. Form factors of block copolymer micelles with spherical, ellipsoidal and cylindrical cores. *J. Appl. Cryst.* **2000**, *33*, 637–640.

(5) Lord Rayleigh, The Incidence of Light upon a Transparent Sphere of Dimensions Comparable with the Wave-Length. *Proc. R. Soc. London A* **1910**, *84*, 25–46.

(6) Guinier, A.; Fournet, G. *Small-Angle Scattering of X-Rays*; John Wiley & Sons: New York, 1955.

(7) Debye, P. Molecular-weight Determination by Light Scattering. *J. Phys. Chem.* **1947**, *51*, 18–32.

(8) Pedersen, J. S.; Svaneborg, C.; Almdal, K.; Hamley, I. W.; Young, R. N. A Small-Angle Neutron and X-ray Contrast Variation Scattering Study of the Structure of Block Copolymer Micelles: Corona Shape and Excluded Volume Interactions. *Macromolecules* **2003**, *36*, 416–433.

(9) Pedersen, J. S.; Gerstenberg, M. C. The structure of P85 Pluronic block copolymer micelles determined by small-angle neutron scattering. *Colloids Surf. A: Physicochem. Eng. Aspects* **2003**, *213*, 175–187.

(10) Derry, M. J.; Fielding, L. A.; Warren, N. J.; Mable, C. J.; Smith, A. J.; Mykhaylyk, O. O.; Armes, S. P. *In situ* small-angle X-ray scattering studies of sterically-stabilized diblock copolymer nanoparticles formed during polymerization-induced self-assembly in non-polar media. *Chem. Sci.* **2016**, *7*, 5078–5090.

(11) Akpinar, B.; Fielding, L. A.; Cunningham, V. J.; Ning, Y.; Mykhaylyk, O. O.; Fowler, P. W.; Armes, S. P. Determining the Effective Density and Stabilizer Layer Thickness of Sterically Stabilized Nanoparticles. *Macromolecules* **2016**, *49*, 5160–5171.

(12) Scattering Length Density. http://gisaxs.com/index.php/Scattering_Length_Density.

(13) The Atomic Scattering Factor Files. http://henke.lbl.gov/optical_constants/asf.html.

(14) Rekveldt, M. T. Novel SANS instrument using Neutron Spin Echo. *Nucl. Instrum. Methods Phys. Res. B: Beam Interact. Mater. Atoms* **1996**, *114*, 366 – 370.

(15) Andersson, R.; van Heijkamp, L. F.; de Schepper, I. M.; Bouwman, W. G. Analysis of spin-echo small-angle neutron scattering measurements. *J. Appl. Cryst.* **2008**, *41*, 868–885.

(16) Washington, A. L.; Li, X.; Schofield, A. B.; Hong, K.; Fitzsimmons, M. R.; Dalgliesh, R.; Pynn, R. Inter-particle correlations in a hard-sphere colloidal suspension with polymer additives investigated by Spin Echo Small Angle Neutron Scattering (SESANS). *Soft Matter* **2014**, *10*, 3016–3026.

(17) Parnell, S. R.; Washington, A. L.; Parnell, A. J.; Walsh, A.; Dalgliesh, R. M.; Li, F.; Hamilton, W. A.; Prevost, S.; Fairclough, J. P. A.; Pynn, R. Porosity of silica Stöber particles determined by spin-echo small angle neutron scattering. *Soft Matter* **2016**, *12*, 4709–4714.

(18) Feigin, L. A.; Svergun, D. I. *Structure Analysis by Small-Angle X-Ray and Neutron Scattering*; Plenum Press: New York, 1987.

(19) Percus, J. K.; Yevick, G. J. Analysis of Classical Statistical Mechanics by Means of Collective Coordinates. *Phys. Rev.* **1958**, *110*, 1–13.

(20) Sears, V. F. Neutron scattering lengths and cross sections. *Neutron News* **1992**, *3*, 26–37.

(21) Brown, D.; Kienzle, P. Neutron activation and scattering calculator. https://www.ncnr.nist.gov/resources/activation/.